

GEOTHERMAL STEAM-WATER SEPARATORS: DESIGN OVERVIEW

Sadiq J. Zarrouk^{1*} and Munggang H. Purnanto²

¹*Department of Engineering Science, The University of Auckland, New Zealand

²Engineering Department, Star Energy Geothermal (Wayang Windu) Ltd., Indonesia

s.zarrouk@auckland.ac.nz

Keywords: *Geothermal Separator, Cyclone, Separator Efficiency, Vertical Separator*

ABSTRACT

Since the development of the liquid dominated geothermal reservoir at Wairakei in 1950's, various separator designs have been utilized to enable the separation of steam and water from two-phase geothermal fluid so that only dry steam is sent to run the turbine and generate electricity. Information from several existing geothermal fields show that there are two common separator designs: the vertical cyclone separator and the horizontal separator. Both designs claim to have high separation efficiency in the order of 99.9% or higher. The vertical cyclone separator is normally found at power stations with strong influence from New Zealand's technology, while the horizontal separator is normally found at power stations with strong influence by Iceland's technology.

This paper reviews the steam-water separator that is commonly used in geothermal steam fields worldwide. Several approaches that can be used to design the geothermal steam-water separator are incorporated. Bangma's and Lazalde-Crabtree's methods are used to design the vertical vessel dimensions whereas Gerunda's method is used to design the horizontal vessel dimensions. The general steps to design the separator for given geothermal fluid data is also presented, starting from selection of separation pressure, predicting the efficiency and calculating the internal pressure drop.

1. INTRODUCTION

The energy from geothermal fluid can be converted into electricity by utilizing the geothermal steam as the working fluid to rotate the turbine which is coupled with the generator. Since turbine design usually requires high steam quality (dryness) at the inlet, the geothermal steam should be as dry as possible or slightly superheated. Even a small quantity of water carried over can cause problems due to the fact that geothermal water contains dissolved minerals (solids) that may form scale deposition on the turbine blades or casing and reduce the conversion efficiency and cause damage to the turbine.

In dry geothermal fields, separators are not required. However, dry steam reservoirs are rare and are found in few areas around the world: Lardarello (Italy), the Geysers (USA), as well as limited dry steam areas in Matsukawa (Japan), Darajat and Kamojang (Indonesia), and Cove Fort Utah (USA) (DiPippo, 2012). Most of the remaining geothermal fields worldwide are liquid-dominated reservoirs producing a mixture of steam and water, therefore a separator is required.

Challenges to develop wet fields for power generation had resulted in the development of steam-water separators. The separator enables the separation of steam and water from two phase geothermal mixtures so that only steam is sent to

run the turbine. Wairakei Geothermal Power Station, New Zealand, was the first plant to use a separator in 1950's. Its successful design was then adopted by many fields around the world with very little change up to present (Foong, 2005).

2. THE GEOTHERMAL SEPARATOR

The earliest method to separate steam and water is by passing the mixture into a large drum, called a knock out drum. Flashing occurs due to the drop in the fluid pressure and the lighter steam will rise up while the heavier water will fall down to the bottom of the drum (Foong, 2005).

Another method to remove water from the mixture is by using a 180° U-bend separator which works through centrifugal effects. This separator is simple in design and is able to remove up to 80% of water. To further increase its dryness, the U-bend separator was installed in series with cyclone separator (Figure 1). However, design quickly excluded the U-bend separator since the cyclone itself is capable of removing almost all of the water.



Figure 1: The U-bend Separator installed together with TOC Separator as seen in the Wairakei Field (Picture by Sadiq Zarrouk, 1997).

Currently, the cyclone separator is the most popular design found in most geothermal power stations around the world. Separation process is carried out by generating centrifugal force on the mixture entering the separator by using a tangential or spiral inlet path to the cyclone. As the fluid rotates, the liquid with higher density will move outward and downwards while the vapour which has lower density will move inward and upward.

The cyclone separator has undergone several improvements to maximise its efficiency. In early designs, the steam was discharged at the top of the vessel while the brine was discharged from the bottom of the vessel (Figure 2). This separator was referred to as top outlet cyclone separator (TOC) also known as the Woods separator. It was designed by Merz and McLellan and is used in some geothermal bores at Wairakei. The performance can be improved by up

to 20% if installed together with U-bend separator (Bangma, 1961).

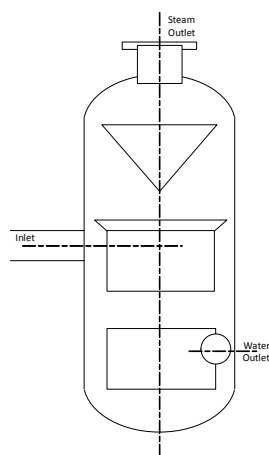


Figure 2: The Top Outlet Cyclone (TOC) Separator (after Bangma, 1961).

Having improved its efficiency, the top outlet cyclone separator was then superseded by the bottom outlet cyclone separator (BOC) also known as the Weber separator. In this design, the steam pipe is placed inside the vessel and leaves from the bottom of the separator. The BOC is popular because of its simplicity and also because separated steam is removed at the bottom of the separator instead of the top. This causes the steam line to support itself on a pipe near ground level making it much simpler than the TOC (Bangma, 1961).

Despite the popularity of the vertical cyclone separator, Povarov et al. (2003; 2005) argued that the new design of horizontal separator developed/used in the Mutnovsky Power Station, Russia has better efficiency and mass-dimension characteristics. The design is based on the experience of designing similar devices in nuclear power stations using the same mechanism for gravitational sedimentation of liquid particles.

During 1967 – 1995, all separators constructed and installed in Iceland were the vertical type. The horizontal type fitted with droplet elimination mats began to gain popularity in later years (Eliasson, 2001). However, there is no detailed publication related to this design. Hence, direct comparison with the vertical design is not possible. The only available practical procedure for horizontal type design was reported by Gerunda (1981) on a liquid-vapour separator. Although some improvements might have made the recent designs slightly different from Gerunda's (1981), the principle of his design is the same as in geothermal separators.

3. GEOTHERMAL SEPARATORS AROUND THE WORLD

The vertical cyclone separator has gained popularity due to its simple design, absence of moving parts, low cost, low pressure drop and high output quality and efficiency (Lazalde-Crabtree, 1984; Hoffmann, 2007). Published data from several geothermal power stations around the world (Table 1) indicates that vertical cyclone separator dominates the design worldwide (Figure 3).

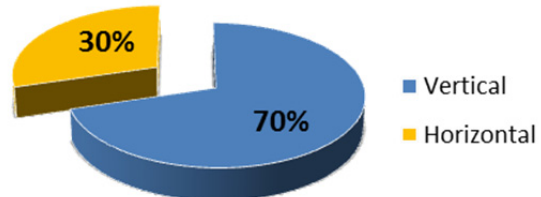


Figure 3: The Distribution of Vertical Separator vs Horizontal Separator Worldwide.

The horizontal separator is used mostly by power plants that inherit the Icelandic technology or was modified from the Russian nuclear industry. The horizontal separator is claimed to be superior to the vertical cyclone separator for the following reasons:

1. The cyclone separation system works effectively only in designed flow regime. Deviation from this regime will affect the load and may lead to deterioration of separation effectiveness and the increase of steam wetness (Povarov et al., 2003; 2005).
2. Water drop in the horizontal separator is at right angle with the steam flow, thus, creating more effective separation process than that of the vertical separator (Moghaddam, 2006).
3. The horizontal separator makes access and service to the measuring equipment easier than the vertical type (Moghaddam, 2006).

Table 1 shows one field (Beowawe) that uses a vertical separator for the high pressure and a horizontal separator for low pressure flash vessel.

Table 1: Geothermal Separators around the World

Country	Field	Unit	Year	Type	MW Rated	Sep. Type	Notes	Ref.	
Costa Rica	Miravalle	Wellhead Unit 1	1995	1-Flash Backpressure	1 × 5	V.	Wellhead unit 1 and wellhead unit 3 have been dismantled in 1998.	(Moya and Nietzen, 2005; Di Pippo, 2008)	
		Wellhead Unit 2	1996	1-Flash	1 × 5	N.A.	There are 7 separation stations that supply the steam needed for Wellhead Unit 1, Unit 1, Unit 2 and Unit 3. Binary plant uses waste brine from Unit 1, 2 and 3.		
		Wellhead Unit 3	1997	1-Flash	1 × 5	N.A.			
		1	1994	1-Flash	1 × 55	V.			
		2	1998	1-Flash	1 × 55	V.			
		3	2000	1-Flash	1 × 29	V.			
		5	2004	Binary	2 × 9.5	V.			
El Salvador	Ahuachapan	1	1975-1976	1-Flash	1 × 30	V.	The horizontal separator in unit 3 is a flasher that is installed to recover low pressure steam from wasted hot water in unit 1 & 2.	(Di Pippo, 1980; Kozaki, 1982; Monterrosa and Lopez, 2010)	
		2	1975-1976	1-Flash	1 × 30	V.			
		3	1980	2-Flash	1 × 35	H.			
El Salvador	Berlin	Wellhead	1992	1-Flash	2 × 5	V.	Wellhead units have been retired.	(Horie, 2001; Di Pippo, 2008; Argueta, 2011; Fuji, 2011)	
		1	1999	1-Flash	1 × 28	V.			
		2	1999	1-Flash	1 × 28	V.			
		3	2006	1-Flash	1 × 40	N.A.			
		4	2007	Binary	1 × 9.2	N.A.			
Indonesia	WayangWindu	1	2000	1-Flash	1 × 110	V.	There are 3 separators for each unit, sized at 40 MW each.	(Murakami et al., 2000; Syah et al., 2010)	
		2	2009	1-Flash	1 × 117	V.			
Indonesia	GunungSalak	1	1994	1-Flash	1 × 55	V.	GunungSalak is also known as Awibengkok.	(Soeparjadi et al., 1998; Di Pippo, 2008; Adiprana et al., 2010)	
		2	1994	1-Flash	1 × 55	V.			
		3	1997	1-Flash	1 × 55	V.			
		4	1997	1-Flash	1 × 55	V.			
		5	1997	1-Flash	1 × 55	V.			
		6	1997	1-Flash	1 × 55	V.			
Mexico	Cerro Prieto I	1 & 2	1973	1-Flash	2 × 37.5	V.	The gathering system consists of cyclone separators at each well, with steam line to power station and brine line to evaporation pond.	(Di Pippo, 2008)	
		3 & 4	1979	1-Flash	2 × 37.5	V.			
		5	1981	2-Flash	1 × 30	V.			
	Cerro Prieto II	1 & 2	1984	2-Flash	2 × 110	V.	The gathering system consists of one pair of wellhead separator and flasher from each well.	(Di Pippo, 2008)	
	Cerro Prieto III	1 & 2	1985	2-Flash	2 × 110	V.			
	Cerro Prieto IV	1-4	2000	1-Flash	4 × 25	V.	The hot brine from the separator is passed to the evaporator section of the hot water binary plant. The dry steam is passed	(Di Pippo, 2008)	
New Zealand	Mokai	1	1999	Flash-Binary	1 × 25, 6 × 5	V.			
		2	2005	Flash-	1 × 34,	V.			

Country	Field	Unit	Year	Type	MW Rated	Sep. Type	Notes	Ref.
				Binary	1×8		into the backpressure steam turbine and delivered to the evaporator section of the binary cycle plant. Mokai 1 has 2 separators while Mokai 2 has only 1 separator.	
New Zealand	Rotokawa	Combined Cycle	1997	Flash-Binary	1×13 , 3×4.5	V.	The dry steam from the separator is sent to the backpressure turbine. The hot brine from the separator is used for the binary plant. The exhaust steam from the turbine is also used for the binary plant.	(Legmann, 1999; Legmann and Sullivan, 2003; Di Pippo, 2008)
		Extension	2003	Binary	1×4.5	N.A.		(Di Pippo, 2008)
		Nga Awa Purua	2010	3-Flash	1×139	V.	Inlet steam pressure: HP=23.5 bara; IP=8.4 bara; LP=2.3 bara.	(Horie, 2009)
New Zealand	Kawerau	1	2008	2-Flash	1×95	V.	Inlet steam pressure: HP=11.3 bara; LP=1.8 bara.	(Horie, 2009)
Iceland	Nesjavellir	1 & 2	1998	1-Flash	2×30	H.	The separation system consists of steam separators and mist eliminators. The brine and exhaust steam from the turbine are both used to heat the water for domestic use in Reykjavic.	(Eliasson, 2001; DiPippo, 2012)
		3	2001	1-Flash	1×30	H.		
		4	2005	1-Flash	1×30	H.		
Iceland	Hellisheidi	1 & 2	2006	1-Flash	2×45	H.	It was initially designed as an electric generating station and then later became a cogeneration heat and power plant. Unit 3 is low pressure turbine, taking advantage of large volume of hot water from Unit 1 & 2 separator. There are three separations stations with 21 water-steam separators in total.	(DiPippo, 2012; Gunnlaugsson, 2012)
		3	2007	1-Flash	1×33	H.		
		4 & 5	2008	1-Flash	2×45	H.		
		6 & 7	2011	1-Flash	2×45	H.		
Iceland	Krafla	1	1978	2-Flash	1×30	V.	Initially, wellhead separators were installed for each well pad. They were replaced with a centralised separation station. Due to ineffectiveness.	(Juliussen et al., 2005)
Iceland	Svartsengi	PP-1	1977	1-Flash	2×1	N.A.	The turbines are the backpressure type.	(Thorolfsson, 2005; Albertsson et al., 2010; DiPippo, 2012)
		PP-2	1981	-	-	-	PP-2 is not used for electricity generation. It is used for district heating with capacity $3 \times 25\text{MW}_{\text{th}}$.	
		PP-3	1981	1-Flash	1×6	V.	The turbine is the backpressure type. The separator is located close to the turbine.	
		PP-4	1989, 1993	Binary	3×1.2 , 4×1.2	N.A.	It was the first time in the world an Ormat's ORC unit was directly connected to a backpressure turbine as a bottoming unit.	

Country	Field	Unit	Year	Type	MW Rated	Sep. Type	Notes	Ref.
		PP-5	1999	1-Flash	1×30	H.	The steam supply system comprises a horizontal separator and a horizontal moisture separator, both with mist eliminator pads.	(Povarov et al., 2003; DiPippo, 2012)
		PP-6	2007	Dry Steam	1×30	-	-	
Russia	Mutnovsky	1	2002	1-Flash	2×25	H.	All equipment except the two-phase pipeline is located inside the building to protect the plant equipment and personnel from the harsh winter weather. One building is used as the power house, while another building is used as a separator building.	(Povarov et al., 2003; DiPippo, 2012)
Russia	Verkhne-Mutnovsky	1	1998	1-Flash	1×4	H.	The separated brine is flashed to be used by steam jet ejectors for non-condensable gas removal. The unique feature of this plant is the use of an air-cooled condenser normally found in a binary plant.	(DiPippo, 2012)
		2 & 3	1999	1-Flash	2×4	H.		
United States of America	Beowawe	1	1985	2-Flash	1×16	V., H.	The vertical separator is used to separate steam and water while the horizontal separator is used as a flasher for the hot brine produced from the vertical one.	(Di Pippo, 2008; DiPippo, 2012)

4. SELECTION OF SEPARATION PRESSURE AND SPECIFICATION

The separation process is simply an application of the first law of thermodynamics of heat and mass balance (Figure 4).

Making a decision on the optimum separation pressure in geothermal power station is not straightforward. Proper understanding of thermodynamics of the conversion process is needed.

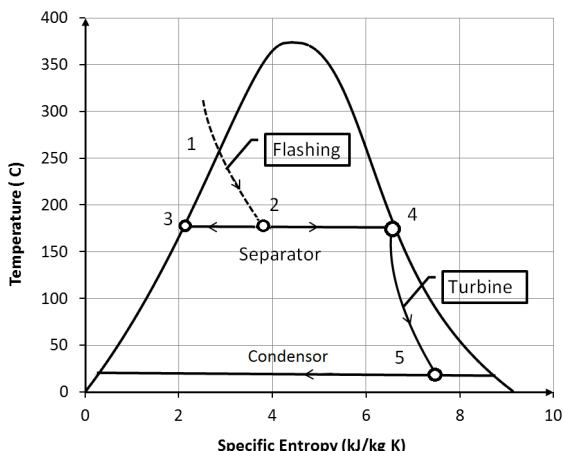


Figure 4: Temperature Entropy Diagram for Typical Single Flash Plant.

Figure 4 shows the geothermal fluid with enthalpy h_1 and mass flow m_f undergoes flashing at constant enthalpy as it travels from the wells to the separator dropping in pressure. Inside the separator saturated water h_3 and saturated steam h_4 is produced (Figure 4). The steam with high enthalpy h_4 is sent to the turbine, while the liquid (brine) with enthalpy h_3 is sent to reinjection wells. By assuming that there is no heat or pressure loss between the separator and the turbine, the inlet steam enthalpy will be equal to h_4 . Hence, the turbine gross mechanical power can be represented mathematically in simplest form as:

$$W = \dot{m}_s \times (h_4 - h_5) \quad (1)$$

$$\dot{m}_s = \frac{(h_2 - h_3)}{(h_4 - h_3)} \times \dot{m}_f \quad (2)$$

Where \dot{m}_s is mass of steam flow rate in kg/s; h is enthalpy in kJ/kg; and W is the power in kW.

Net electrical power can be calculated by including generator efficiency in equation 1 after considering the effect of non-condensable gases (NCG) and parasitic load.

For geothermal resource with certain mass flow rate and enthalpy, equations 1 and 2 shows that the produced turbine output is influenced by the separator pressure and so in order to get the optimum pressure, the turbine output should be calculated for various separation pressures. The separator pressure which gives the maximum turbine output will be selected as the optimum pressure (Figure 5). The same principle applies for double flash and triple flash plants.

It is important to note that: the curve in Figure 5 is very flat near optimum conditions, so other criteria might also be considered in finally setting the separation pressure.

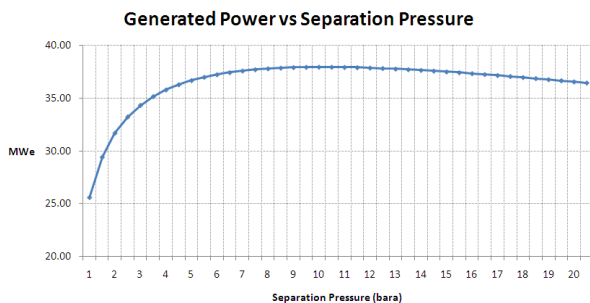


Figure 5: Generated Power for Several Separation Pressure ($h = 1600 \text{ kJ/kg}$, mass flow = 711.4 t/h).

4.1 Silica Scaling Consideration

Dissolved silica (SiO_2) is the common mineral found in geothermal fluid which can cause scaling problems in steam field equipment, especially in separators, brine pipelines and reinjection wells. Silica can exist as amorphous silica or quartz with its own solubility characteristic. The solubility in the hot reservoir fluid is controlled by quartz (Fournier, 1986) whereas at the surface is controlled by the solubility of amorphous silica (Fournier and Rowe, 1977) (see Figure 6).

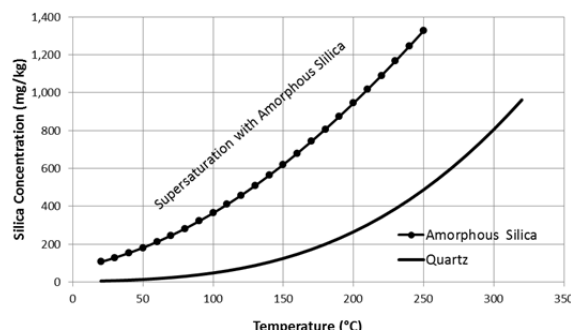


Figure 6: Temperature dependence of the solubility of quartz and amorphous forms of silica (after, Fournier and Rowe, 1977 and Fournier, 1986).

Since silica is dissolved in liquid, as the geothermal fluid is flashed, its concentration increases in the geothermal brine due to the loss of steam. Further flashing will result in higher silica concentration in the brine, resulting in high probability of scaling problems. .

To predict the probability of scaling occurrence, silica saturation index (SSI) is used. SSI is the ratio of measured silica concentration in solution to the equilibrium solubility of amorphous silica at the same pH and temperature. Saturation occurs when SSI is equal to one. When SSI is less than one, there will be less risk of silica deposition, whereas when SSI is greater than one, there will be higher risk for silica deposition.

The SSI should be considered when setting the optimum separation pressure. Based on field experience, Barnett (2007) recommended a $1.15 \leq \text{SSI} \leq 1.3$ for single flash and $1.3 \leq \text{SSI} \leq 1.5$ for double flash plants/separators. Therefore, adjustment on selected optimum pressure might be required to reduce the value of SSI and minimise scaling. If

adjustment does not give significant effect, other scaling prevention techniques should be considered (e.g. acidizing).

It should be noted that silica scaling cannot be prevented 100%, even with $\text{SSI} \leq 1$, but the above criteria will result in small amount/rate of scaling which is manageable. Silica scaling has been reported to take place mainly in the bottom of separators and water (brine) drums in several geothermal developments (Adiprana, et al, 2010; Tassew, 2001; Grassiani, 2000; Delliou, 1989).

Villasenor and Calibugan (2011) reported silica scaling on the walls of the inlet nozzle of the separator at the Tiwi geothermal field in the Philippines.

Scaling will affect the efficiency and performance of the separator by reducing the available internal volume of the separator through the build-up of scale. This will hinder the flow of brine, reducing steam quality (increase in carry over) and can result in separator flooding.

5. METHODS OF SEPARATOR SIZING

The liquid-vapour separation process involves a combination of the following mechanisms: gravity settling, centrifugal impact, flow-line interception, diffusion deposition, electrostatic attraction, thermal precipitation, flux forces and particle agglomeration techniques (Lee, 1995). Most separators rarely operate solely with a single mechanism, although one mechanism may dominate (Lee, 1995). The vertical cyclone separator and horizontal separator work on different mechanisms. Centrifugal action is the dominant mechanism for the vertical cyclone separator, while gravity settling is the dominant mechanism for a horizontal separator.

All fluid entering the separator is a mixture of water and vapour. Understanding of two phase flow behaviour is necessary as it is strongly linked to the separation efficiency (White, 1983).

Two-phase fluid can form different flow regimes inside geothermal pipelines as shown in Figure 7. The bubble flow is formed if there are bubbles of steam/gas that moves at approximately the same velocity as the liquid, but at the upper part of the pipe. The plug flow is formed if there are alternating plugs of liquid and gas that move at the upper part of the pipe. The stratified flow is formed when the liquid travels at the low part of the pipe, while the gas travels in the upper side of the pipe and both are separated by a smooth liquid-gas interface. The wave flow is similar to the stratified flow but the gas moves at a higher velocity and the liquid-gas interface is disturbed by waves travelling in the flow direction. The slug flow is formed if the wave of the liquid is picked up by the more rapidly moving gas to form a frothy slug which passes through the pipe at much greater velocity than the average liquid velocity. The annular flow is formed when the gas flows at high velocity at the centre of the pipe surrounded by the film of liquid flow inside the pipe wall. The mist flow is formed when most or nearly all of the liquid is entrained as spray by the gas (Harrison, 1975).

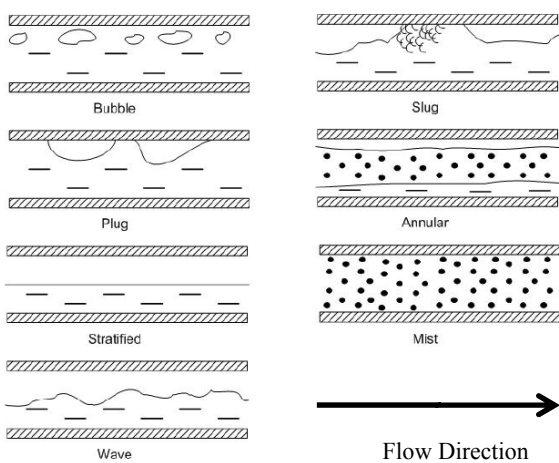


Figure 7: Two-Phase Flow Patterns in Horizontal Flow.

(After Harrison, 1975; Allen, 1977)

Slug flow is not desired due to the high pressure drop, vibration and its potential to create problems for the piping support. Annular flow is desirable from the standpoint of pipe restraint and low pressure drop (Darmawan, 1988).

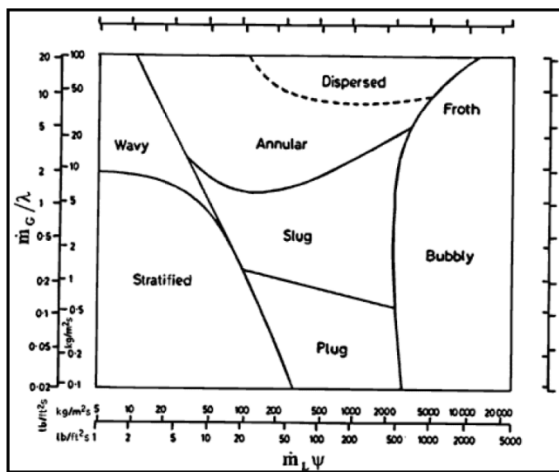


Figure 8: Baker's Map (from Thome, 2010).

Predicting the fluid flow accurately is difficult. Some methods have been developed and most are presented in two dimensional flow pattern maps. One map that is commonly used is the Baker map shown in Figure 8 (Allen, 1977). The Baker map was derived using the mass velocity of the liquid and gas by including parameters λ and ψ (Thome, 2010) given by the following equations:

$$\dot{m}_{VL} = \frac{\dot{m}_L}{A} \quad (3)$$

$$\dot{m}_{VG} = \frac{\dot{m}_G}{A} \quad (4)$$

$$\lambda = \left(\frac{\rho_G}{\rho_{air}} \times \frac{\rho_L}{\rho_{water}} \right)^{1/2} \quad (5)$$

$$\psi = \left(\frac{\sigma_{water}}{\sigma} \right) \left[\left(\frac{\mu_L}{\mu_{water}} \right) \left(\frac{\rho_{water}}{\rho_L} \right)^2 \right]^{1/3} \quad (6)$$

Where ρ_G , ρ_L , μ_L and σ are properties of the fluid and the reference properties are $\rho_{water} = 1000 \text{ kg/m}^3$; $\rho_{air} = 1.233 \text{ kg/m}^3$; $\mu_{water} = 0.001 \text{ Ns/m}^2$; $\sigma_{water} = 0.072 \text{ N/m}$.

Another commonly used flow pattern map is the one proposed by Mandhane et al. (1974) as shown in Figure 9. Mandhane et al. (1974) developed the map as improvements to the previously available maps. The main advantage of this map is its simplicity, since it is based on the superficial velocities of the two fluids. The map also needs to be adjusted for the specific characteristics of the fluids, though.

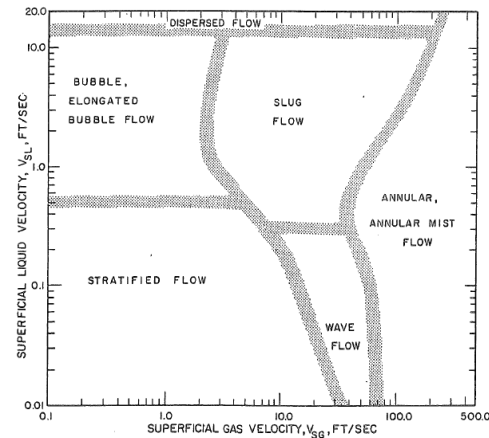


Figure 9: Mandhane's Map (from Mandhane et al., 1974).

However, experience has shown that no single pattern map works for all ranges of pipe diameter. Although a newer map, like Mandhane et al. (1974), was developed from a wider range data, however it does not perform well in pipes of larger diameters.

5.1 Sizing Horizontal-Type Separators

Horizontal separators are mainly flash vessels where the mixture fluid enters from one top end of the vessel and travels horizontally while flashing occurs. Water will move downward due to gravity while steam flows from another top connection at the opposite side of the inlet (Figure 10). A ball check vessel is usually installed at the steam outlet to avoid water flooding the dry steam line. The chief concern is to have the mixture velocity sufficiently lowered to give the liquid particles enough time to settle before the steam leaves the vessel from the top (Gerunda, 1981).

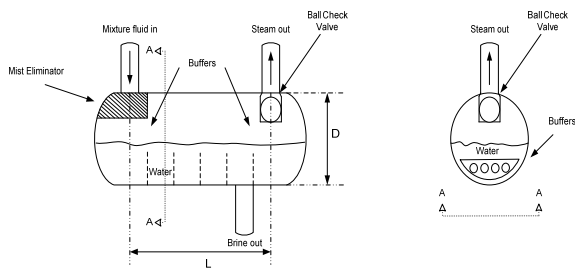


Figure 10: Dimensions for Horizontal Separator (After Gerunda, 1981).

The two parameters concerned with horizontal separator design are mixture fluid velocity and gas residence time. Both are functions of vessel diameter. Gerunda (1981) suggested that the following points should be followed:

- The maximum liquid level will not exceed 0.3048 meters from the top of the vessel but will not drop below the centre-line of the separator.
- The volume of vessel dished heads is not taken into account in vessel sizing calculations.
- Inlet and outlet nozzles shall be located as close as practical to the vessel tangent lines.
- Liquid outlets shall have anti-vortex baffles.

Some parameters must be considered for designing a horizontal separator. The parameters are terminal velocity, vapour velocity in the horizontal direction and the holding time. Gerunda (1981) proposed two approaches for the sizing of the horizontal vessel; by liquid separation and by the holding time.

For a given two-phase flow, the first step is to determine the terminal velocity (v_t) as a function of liquid density (ρ_L) and vapour density (ρ_v) using equation 7 below. K' is a constant value based on gravity, droplet diameter and the drag coefficient of a liquid particle. For most systems, K' ranges between 0.1 and 0.35. Gerunda (1981) recommended the value for K' to be 0.227 except when special considerations are warranted. This value is dimensionless and should be used in equation 7 with the following fluid properties: ρ_L and ρ_v in lb/ft³, resulting v_t in ft/s.

$$v_t = K'[(\rho_L - \rho_v)/\rho_v]^{1/2} \quad (7)$$

By calculating the gas residence time and equating it with the time required for the liquid particles to settle out at the terminal vapour velocity, equation 8 is obtained and can be used to set the vessel diameter.

$$D = \left[\frac{f_{hv} V}{(L/D)(\pi/4)f_{av}v_a} \right]^{1/2} \quad (8)$$

where, V is the volumetric flow rate (ft³/s); f_{hv} is the fraction of height; f_{av} is the fraction of area; v_a is the allowable vapour velocity (ft/s); D is the diameter of vessel (ft); and L is the length of the vessel (ft).

From experience, Gerunda (1981) recommended the allowable vapour velocity (v_a) to be 15% of the calculated terminal velocity (v_t) to ensure acceptable liquid disentrainment during normal flow surges. However, this recommendation may be neglected (i.e. $v_a = v_t$) if the mist eliminator is installed inside the separator which results in a smaller vessel diameter.

Trial and error will be required to solve equation 8. Gerunda (1981) proposed a general guideline for L/D ratio as given in Table 2, after considering economics and layout restrictions. Another assumption that can be made is by setting the liquid level at the centre of the separator, so that $f_h = f_a = 0.5$.

Table 2: L/D Ratio for Different Pressure (modified from Gerunda, 1981)

Operating Pressure (Barg)	L/D ratio
0 – 17.24	3.0
17.31 – 34.47	4.0
34.54 and higher	5.0

When the horizontal separator size is set by the holding time of the liquid, the diameter of the horizontal vessel must be determined from trial and error. To solve this problem, the following approach can be used: considering the holding time (t_h) formula as given by equation 9, a new fraction area, f_{al} , is introduced and defined as the fraction of area occupied by the liquid. Rearranging this equation to solve for D , Equation 10 is obtained. Using the L/D ratio from Table 2, D can be calculated.

$$t_h = \frac{(\pi/4)D^2 f_{al} L}{V_l} \quad (9)$$

$$D = \left[\frac{t_h V_l}{(L/D)(\pi/4)f_{al}} \right]^{1/3} \quad (10)$$

where V_l is volumetric flow rate of the liquid (ft³/s), f_{al} is the fraction area occupied by the liquid, t_h is the liquid holding time (s), D is the diameter of vessel (ft); and L is the length of vessel (ft).

5.2 Sizing Vertical-Type Separators

The fundamental principle of a vertical cyclone separator is to create a vortex that will centrifuge the liquid to the vessel walls, letting the steam concentrate in the middle. Under gravity, the liquid at the walls will move down and be collected at the bottom of the vessel, while the steam will enter the middle tube and will be directed to leave the vessel through the bottom pipe (Figure 11).

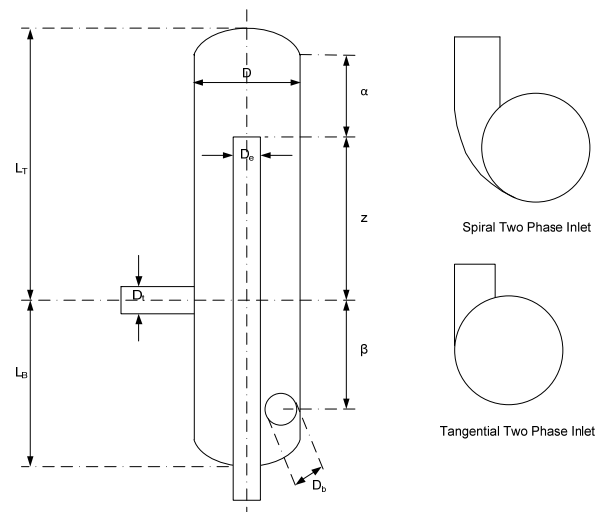


Figure 11: Vertical BOC Separator (Bangma 1961; Lazalde-Crabtree, 1984).

Leith and Licht (1972) suggested that the efficiency of a cyclone separator depends on three dimensionless parameters: C , a cyclone design number depending upon the physical shape (not size); ψ' , a modified type of impaction parameter depending upon operating condition; and n , the exponent in the modified form of the vortex law for tangential velocity distribution. Leith and Licht's (1972) approach was based on the concept of continual radial backmixing of the uncollected particles, coupled with the calculation of an average residence time for the gas in a cyclone separator having a tangential inlet. Leith and Licht's (1972) work was developed for a de-duster and later

modified by Lazalde-Crabtree (1984) for a geothermal vertical cyclone separator.

Both the Bangma and Lazalde-Crabtree methods can be used to design the dimensions of the vertical cyclone separator. The vessel dimensions are all given in terms of diameter of the inlet pipe. The calculation of inlet pipe size (diameter) is given as follows:

$$A = \frac{Q_{VS}}{v_t} \quad (11)$$

$$D_t = \left[\frac{4A}{\pi} \right]^{1/2} \quad (12)$$

where A is the surface area; Q_{VS} is the volumetric steam flow; and D_t is the inlet pipe diameter. Figure 11 and Table 3 show the recommended size of the vertical vessel.

Table 3: Vertical Bottom Outlet Cyclone Separator Dimension to be used with Figure 11

Parameter	Bangma (1961)	Lazalde-Crabtree (1984)
D	$3 D_t$	$3.3 D_t$
D_e	$0.8 D_t^*$ or $1 D_t^{**}$	$1 D_t$
D_b	$1 D_t$	$1 D_t$
α	<i>Not specified</i>	$-0.15 D_t^{***}$
β	$3 D_t$	$3.5 D_t$
Z	$3D_t^*$ or $4 D_t^{**}$	$5.5 D_t$
L_T	$7 D_t$	Not specified
L_B	$4.5 D_t$	Not specified
A_o	Circle; $A_o = \frac{1}{4}\pi D_t^2$	Rectangle; $A_o = A_e \cdot B_e$

D_t is inlet pipe diameter

*Tangential inlet; **Spiral inlet; ***The value is negative because of the nomenclature (inside the head).

5.2 Separator Efficiency

The separator performance is a measure of the proportion of brine that is carried over with the steam:

$$\eta_s = \frac{\dot{m}_s}{\dot{m}_b + \dot{m}_s} \times 100 \quad (13)$$

where η_s is the separator efficiency, \dot{m}_s and \dot{m}_b are the steam flow rate and brine carryover in t/h respectively.

Typical efficiency ranges between 99.5% and 99.99%. Higher efficiency would be preferable so that more steam is sent to run the turbine which is then converted into electricity and also less/minimum silica scaling problems in the turbines. However, practical experience has shown that, a perfect 100% efficiency ($\dot{m}_b = 0$) should not be expected.

It is not practically possible to directly measure the brine carryover (\dot{m}_b) to calculate the separator efficiency (equation 13). This is because it is a small component of steam flow and also it is masked (diluted) by condensate forming in the steam pipeline as the pipelines loses heat.

However, the carryover can be measured indirectly using the chemical signature of the geothermal brine namely Sodium (from the Author experience), other natural tracers like Chloride can potentially be used. The principle is that carryover from the separator introduces sodium into the steam pipelines. Measuring the concentration of sodium in the separated steam can be used to calculate the brine carryover:

$$\dot{m}_b = \frac{\dot{C}_s^{Na}}{C_{sb}^{Na}} \quad (14)$$

where C_{sb}^{Na} in the concentration of sodium in separated brine in g/t.

White (1983) proposed a similar equation for calculating separation efficiency from the ratio of outlet purity to the inlet purity, where steam purity is defined as the total dissolved (TDS) solids in the steam. The correlation can be shown as follows:

$$Sp = \frac{\dot{C}_s^{Na}}{C_{sb}^{Na}} \times TDS \quad (15)$$

$$\eta_s = \left[1 - \frac{\dot{C}_s^{Na}}{C_{sb}^{Na}} \right] \times 100 \quad (16)$$

where TDS is the Total Dissolved Solids in the brine (ppm), Sp is the separated water purity.

The natural tracer concentration is normally measured in a drain pot following the separator. Note that isokinetic probes normally installed near the power station may not be suitable for sampling for sodium because of the low sodium concentration by the time the steam reaches the station. This is due to scrubbing effects in multiple drain pots and/or potentially injection of wash water if large scrubbers near the power stations are used.

However, White's method (1983) can be used once the separators have been put into operation to inspect the actual performance. At the initial stage of design, an empirical approach is preferred.

The most popular empirical approach to estimate the efficiency of a geothermal vertical cyclone separator is the one proposed by Lazalde-Crabtree (1984). Lazalde-Crabtree (1984) defines the separator (theoretical) efficiency as a product of centrifugal efficiency and entrainment efficiency.

$$\eta_{eff} = \eta_m \cdot \eta_A \quad (17)$$

where: η_{eff} is the effective efficiency; η_m is the centrifugal efficiency; and η_A is the entrainment efficiency.

Foong (2005) effectively related the difference between the theoretical efficiency (η_{eff}) and the actual efficiency (η_s) to water creep along the vessel walls.

The centrifugal efficiency (η_m) that reflects the operating condition inside the cyclone is strongly influenced by the diameter of drop particles (d_w) and the tangential inlet velocity of the steam (u) as given in equations 18 to 25 below:

$$\eta_m = 1 - EXP \left[-2(\psi' C)^{\frac{1}{2n+2}} \right] \quad (18)$$

where C is a dimensionless parameter given by equation 19; n is a dimensionless free vortex law coefficient given by equation 20 and ψ' is the centrifugal inertia impaction parameter given by equation 25.

$$C = \frac{8 K_c D^2}{A_o} \quad (19)$$

$$\frac{1 - n_1}{1 - n} = \left(\frac{294.3}{T + 273.2} \right)^{0.3} \quad (20)$$

where K_c is a dimensionless parameter given by equation 21, A_o is the inlet shape area; T is the saturated temperature; n is a parameter determined from equation 20 when $n_1 = 0.6689 D^{0.14}$.

$$K_c = \frac{t_r Q_{VS}}{D^3} \quad (21)$$

where t_r is the residence time, obtained from the following equation:

$$t_r = t_{mi} + \frac{t_{ma}}{2} \quad (22)$$

where t_{mi} is the average minimum residence time of steam inside the vessel and t_{ma} is the maximum additional time of steam inside the cyclone as given by equation 23 and 24 respectively.

The centrifugal inertial impaction is very sensitive to the drop diameter of water particle as shown in equation 25 below:

$$\psi' = \frac{\rho_w d_w^2 (n + 1) u}{18 \mu_v D} \quad (25)$$

where μ_v is the steam viscosity and u is the inlet steam velocity derived from equation 26.

$$u = \frac{Q_{VS}}{A_o} \quad (26)$$

Determination of the drop particle size was accomplished by Lazalde-Crabtree using the basic equation developed by Nukiyami-Tanasawa combined with the data obtained from actual well-head separators (Lazalde-Crabtree, 1984). Lazalde-Crabtree's (1984) final formula is given by equation 27.

$$d_w = \frac{66.2898}{v_t^a} \sqrt{\frac{\sigma_L}{\rho_L}} + B \cdot (1357.35) \left[\frac{\mu_L^2}{\sigma_L \rho_L} \right]^{0.2250} \times \left(\frac{Q_L}{Q_{VS}} \right)^{0.5507} \times v_t^e \quad (27)$$

Equation 27 should be used with the following dimensions: ρ_L in g/cm^3 , v_t in m/s , σ_L in dyne/cm , μ_L in poise, Q_L and Q_{VS} in m^3/s , resulting in d_w in microns.

The variables a , B , and e are dependent on the type of two-phase flow pattern according to Baker's map and are given in the Table 4.

$$t_{mi} = \frac{V_{OS}}{Q_{VS}} \quad (23)$$

$$t_{ma} = \frac{V_{OH}}{Q_{VS}} \quad (24)$$

V_{OS} and V_{OH} are the volume of steam inside the vessel given by Figure 12.

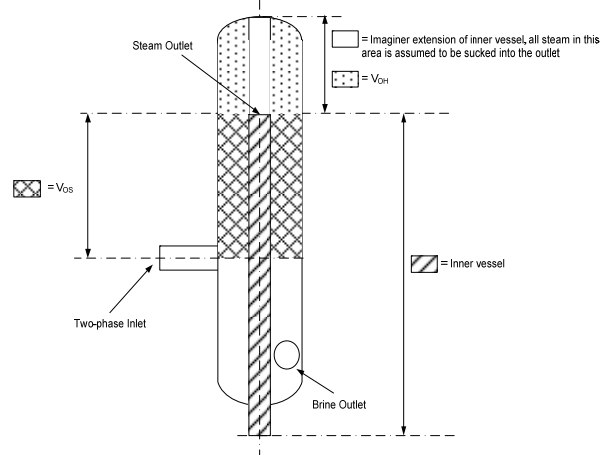


Figure 12: V_{OS} and V_{OH} Calculation (from Lazalde-Crabtree, 1984).

Table 4: Variables a , B , e used with equation 27 (from Lazalde-Crabtree, 1984)

Type of 2-Phase Flow Pattern	a	B	e
Stratified and Wavy	0.5436	$94.9042 (X_i)^{-0.4538}$	0.0253
Annular	0.8069	$198.7749 (X_i)^{0.2628}$	-0.2188
Dispersed & Bubble	0.8069	$140.8346 (X_i)^{0.5747}$	-0.2188
Plug and Slug	0.5436	$37.3618 (X_i)^{-0.0000688}$	0.0253

To calculate the surface tension of water as function of temperature, the following approach can be used (Vargaftic et al., 1983):

$$\sigma = Y \left[\frac{T_c - (T + 273.15)}{T_c} \right]^k \times \left[1 + b \left(\frac{T_c - (T + 273.15)}{T_c} \right) \right] \quad (28)$$

where $T_c = 647.15 \text{ K}$; $Y = 235.8 \times 10^{-3} \text{ N/m}$; $b = -0.625$; $k = 1.256$; resulting in σ in N/m .

The entrainment efficiency (η_A) is function of annular steam velocity given by equations 29 to 31.

$$\eta_A = 10^j \quad (29)$$

$$j = -3.384 (10^{-14}) (V_{AN})^{13.9241} \quad (30)$$

$$V_{AN} = \frac{4Q_{VS}}{\pi(D^2 - D_e^2)} \quad (31)$$

where the range of η_A should be $0 \leq \eta_A \leq 1$.

The pressure drop can be expressed as:

$$\Delta P = \frac{(NH)u^2\rho_v}{2} \quad (32)$$

$$NH = 16 \frac{A_o}{D_e^2} \quad (33)$$

where ΔP is the steam pressure drop; u is the tangential inlet velocity; ρ_v is the mass density of vapour; A_o is the inlet shape area; and D_e is the steam outlet pipe diameter.

5.3 Effect of Inlet Nozzle Design on BOC Separator Performance

The cross section of the cyclone separator inlet can be circular, square or rectangular. A circular inlet is simple in construction due to the fact that the two phase pipe can be used directly as the entry point of the cyclone separator. In contrast, a rectangular inlet requires a circular to rectangular transition piece, located fairly close to the cyclone body. Design of this transition piece must be done carefully to create a smooth transition process. Improper design may lead to boundary layer separation and extra turbulence in the incoming flow (Hoffmann, 2007). A rectangular inlet is preferred by some designers as it joins the body of the cyclone smoothly.

The quality of separation for vertical BOC separator is influenced by the flow conditions that exist at the inlet. As the inlet velocity increases, the output steam wetness will decrease until it reaches a certain point where the output steam wetness increases drastically (Lazalde-Crabtree, 1984). This point is called the breakdown velocity and is shown in Figure 13 which demonstrates that the breakdown velocity is approximately 42 m/s. As the inlet velocity reaches this point, the outlet steam quality suddenly decreases with very high slope.

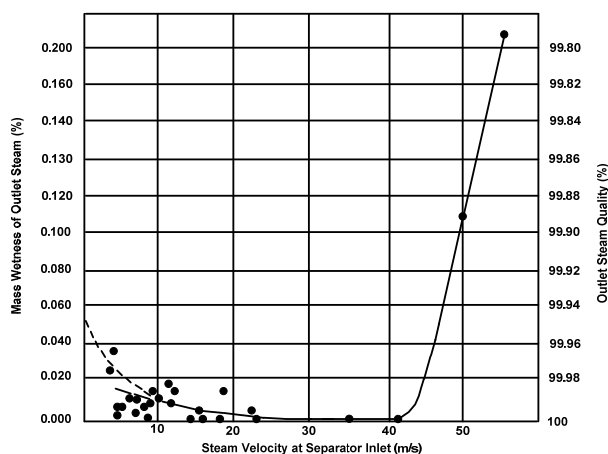


Figure 13: Separator Performance (from Lazalde-Crabtree, 1984).

The highest efficiency is achieved when the inlet velocity is between 30 m/s to 40 m/s. The challenge which arises is how to keep the inlet velocity within this range and just below the breakdown velocity in order to achieve the highest possible efficiency. Controlling the fluid velocity exactly at the entrance of the vessel with minimum disturbance to the incoming fluid is not practical. Hence, the only method is by designing the inlet shape geometry in such a way that the fluid velocity at the upstream pipe will remain the same as the velocity at the entrance of the cyclone body.

There are two types of separators inlet: tangential inlet and scroll inlet. The scroll inlet is superior as it provides a smoother aerodynamic transition resulting in improved separation efficiency (Hoffmann, 2007; Pointon et al., 2009). In addition, the scroll inlet produces an effect upon cyclone performance which is similar to that produced by increasing the body diameter. This brings about an increase in incoming angular momentum (Hoffmann, 2007).

5.4 Other Design Features

An important requirement for separator design is the pressure drop within the vessel. Good separator design will have low pressure drop which will result in lower enthalpy loss. Hence, more energy is sent to the turbine. The BOC separator has a lower pressure drop (equations 32 and 33) compared with the TOC (Figure 2) and earlier combined U-bend - TOC design shown in Figure 1.

The brine leaving the separator (outlet) is normally connected to a water drum (pressure vessel) immediately after the separator to help control water level inside the separator, to help form a seal against steam loss and help dampen flow/pressure surges. The water drum can be either vertically or horizontally mounted next to the separator. Early well head separators (e.g. Wairakei) had a small horizontal water drum connected to it. As the separator size increased, vertical water drums were used which gave more water level control (e.g. Wairakei and Ohaaki). Later as the separators became more centralised and larger in size, large horizontal water drums were used (e.g. Mokai, Rotokawa, Te Huka). Some of the more recent separators designs use built-in water storage by extending the height of the separator (e.g. the 159 MWe Te Mihi power station, New Zealand) or having the lower section of the separator larger in diameter than the upper section (e.g. the 140 MWe Nga Awa Purua power station, New Zealand).

The detailed mechanical design of the separator is outside the scope of this work, but it mainly follows pressure vessel design standards. However, main features include: minimum of 3 mm corrosion/erosion allowance (~0.1 mm/year) on the steel walls thickness, lifting and handling mounts, manholes for access during cleaning. The separator vessel requires deep foundation to support its weight when full of water. It is not allowed to move due to thermal expansion and is secured against earthquakes.

The separators are thermally insulated with fiberglass or calcium silicate insulation to minimise heat loss and the condensation of steam which can result in drop in efficiency. The insulation material is normally covered in aluminium cladding to contain and protect it from rain and other weather elements.

Several authors have proposed or developed new separator designs including:

- Jung and Wai (2000) developed a Boundary Layer Inline Separator Scrubber (BLISS), which is horizontal multi-positional centrifugal separator, which can save 50% in cost and 75% in the overall pressure drop. A horizontal in-line centrifugal separator was trialled at Wairakei, New Zealand in the 1950s (Brian White private communications).
- Foong (2005) proposed a new TOC design that minimise water creep, reduce pressure drop, improve settling efficiency and improve access to the inside of the separator.

However none these designs has made it to commercial use with geothermal steam plants and it is likely that the BOC and the horizontal separators will remain the main two designs used in the foreseen future.

6. CONCLUSION

Steam-water separators have enabled the utilization of liquid dominated reservoir for electricity generation. High separation efficiency is sought, as it results in high turbine output, long life of turbine blades and low maintenance cost.

Separator pressure is chosen through optimum power output calculations while minimising and preventing silica scaling. Amorphous silica has been reported to deposit mainly at the bottom of the separator vessel.

The vertical cyclone separators and the horizontal separators are the two popular designs adopted widely for geothermal application. Based on the reported data; 70% of power plants use vertical separators while 30 % use horizontal separators.

The basic design calculations for sizing the different types of separator are summarised in this work and the advantages and the disadvantages of the different designs are also outlined.

The selection of the design is mostly based on the preference and the experience of the plant owner/operator or the technology provider.

The vertical BOC separator with spiral inlet is the most common design currently used by the industry, while the TOC and the tangential inlet separators are no longer being used.

The calculated efficiency of the BOC separator typical ranges between 99.5% and 99.99 %, by maintaining an inlet velocity between 30 m/s to 40 m/s. Actual efficiency can be measured indirectly after construction of the separator using chemical sampling methods.

It is acknowledged that the actual separator efficiency η_s is less than the calculated/effective efficiency η_{eff} and some brine carryover will take place.

ACKNOWLEDGEMENTS

The authors would like to thank the Indonesian Geothermal Association for the kind permission to reproduce the manuscript, Hind Behaya for her help in reformatting the manuscript and finally Brian White for his valuable comments and for reviewing the manuscript.

REFERENCES

Adiprana, R., Izzuddin, E., Yuniaro: Gunung Salak Geothermal Power Plant Experience of Scaling/Deposit: Analysis, Root Cause and Prevention. *Proceedings World Geothermal Congress 2010*, Bali, Indonesia, (2010).

Albertsson, A., G., Porolfsson, J., Jonsson: Three Decades of Power Generation-Svartsengi Power Plant. *Proceedings World Geothermal Congress 2010*, Bali, Indonesia (2010).

Allen, M. D.: Geothermal Two-Phase Flow: *A Study of the Annular Dispersed Flow Regime*. A Thesis presented for the Degree of Doctor of Philosophy, University of Auckland, (1977).

Argueta, G. G. M.: *Operation and Maintenance of High Temperature Geothermal Wells*. Short Course on Geothermal Drilling, Resource Development and Power Plants, Santa Tecla, El Salvador, United Nations University Geothermal Training Programme, (2011).

Bangma, P.: The Development and Performance of a Steam-Water Separator for Use on Geothermal Bores. *Proceedings of the U.N. Conference on New Sources of Energy Rome 1961 Vol. 3 (Issue G/13): 60 – 77*, (1961).

Darmawan: *Wellhead Separator Design for Wells DNG-7, DNG-8 and DNG-13 in Dieng Geothermal Field in Indonesia*. Project Report of Geothermal Institute. New Zealand, The University of Auckland, (1988).

Barnett, P. *Cost of Geothermal Power in NZ: 2007 Update*. New Zealand Geothermal Association Seminars, Auckland, November (2007). <http://www.nzgeothermal.org.nz/publications/Reports/Workshop2007/GeothermalCosts2007.pdf>

Di Pippo, R.: Ahuachapan Geothermal Power Plant, El Salvador. *Proceedings of the Fourth Annual Geothermal Conference and Workshop, Santa Cruz, California, Electric Power Research Institute*, (1980).

DiPippo, R.: *Geothermal Power Plants Principles, Applications, Case Studies and Environmental Impact*. Second Edition. United Kingdom, Elsevier Ltd, (2008).

DiPippo, R.: *Geothermal Power Plants: Principles, Applications, Case Studies and Environmental Impact*. Third Edition. United States of America, Elsevier Ltd, (2012).

Eliasson, E. T.: Power Generation from High-Enthalpy Geothermal Resources. *GHC Bulletin (June)*, (2001).

Foong, K. C.: Design Concept for a More Efficient Steam-Water Separator. *Proceedings World Geothermal Congress*. Antalya, Turkey, (2005).

Fuji: *Consulting Service Report for Investigation of Berlin Geothermal Power Plant in Republic of El*

Salvador. Fuji Electric System Japan Consulting Institute, (2011).

Gerunda, A.: How to size liquid-vapor separators. *Chemical Engineering May* 4: 81 – 84, (1981).

Gunnlaugsson, E.: *The Hellisheiði Geothermal Project - Financial Aspects of Geothermal Development*. Short Course on Geothermal Development and Geothermal Wells. Santa Tecla, El Salvador, UNU-GTP and LaGeo, (2012).

Harrison, R. F.: *Methods for the Analysis of Geothermal Two-Phase Flow*. Thesis submitted as a requirement for the Degree of Master of Engineering, University of Auckland: 204, (1975).

Hoffmann, A. C., L.E. Stein: *Gas Cyclones and Swirls Tubes Principles, Design and Operation*. 2nd Edition. New York, Springer, (2007).

Horie, T.: Berlin Geothermal Power Plant. *Fuji Electric Review Vol. 47 (No. 4)*: pp. 108-112, (2001).

Horie, T.: Kawerau and Nga Awa Purua Geothermal Power Station Projects, New Zealand. *Fuji Electric Review Vol. 55 (No. 3)*: pp. 80-86, (2009).

Juliusson, B. M. B., Palsson, A., Gunnarsson: Krafla Power Plant in Iceland - 27 Years of Operation. *Proceedings World Geothermal Congress*, Antalya, Turkey, (2005).

Jung, D. B. and Wai, K. K. BLISS: Boundary Layer Inline Separator Scrubber, *Proceedings World Geothermal Congress*, Kyusu -Tohoku, Japan May28 - June 10, (2000).

Kozaki, K.: Fuji Geothermal Power Plant. *Fuji Electric Review Vol. 28 (No. 4)*, (1982).

Lazalde-Crabtree, H.: Design Approach of Steam-Water Separators and Steam Dryers for Geothermal Applications. *Geothermal Resources Council Bulletin(September)*: 11 – 20, (1984).

Lee, K. C.: Performance of A Model In-Line Vortex Separator. *World Geothermal Congress*. Florence, Italy, (1995).

Lee, K. C.: Performance Tests of the Condensate drian Pots at Wairakei. *Proceedings of the Pacific Geothermal Confrence*, New Zealand. 123-129. (1982)

Legmann, H.: Rotokawa Geothermal Combined-Cycle Power Plant. *Bulletin d'Hydrogeologie No. 17*, (1999).

Legmann, H. and P. Sullivan: The 30 MW Rotokawa I Geothermal Project Five Years of Operation. *International Geothermal Conference*. Reykjavic, (2003).

Leith, D. and W. Licht: The Collection Efficiency of Cyclone Type Particle Collectors. A New Theoretical Approach. *AICHE Symps. Series Vol. 68 (No. 126)*: 196 – 206, (1972).

Mandhane, J. M., G. A., Gregory, K., Aziz: A Flow Pattern Map for Gas-Liquid Flow in Horizontal Pipes. *Int. J. Multiphase Flow Vol. 1*: 537 – 553, (1974).

Monterrosa, M. and F. E. M., Lopez: Sustainability Analysis of the Ahuachapan Geothermal Field: Management and Modelling. *Geothermics* 39: 370 – 381, (2010).

Moya, P. and F., Nietzen: First Ten Years of Prooduction at the Miravalles Geothermal Field, Costa Rica. *Proceedings World Geothermal Congress 2005*, Antalya, Turkey, (2005).

Moghaddam, A. R.: *A Conceptual Design of A Geothermal Combined Cycle and Comparison with A Single-Flash Power Plant For Well NWS-4, Sabalan, Iran*. Project Report of Geothermal Training Programme, The United Nations University, Iceland, No. 18, (2006).

Murakami, H., Y. Kato and N. Akutsu: Construction of the Largest Geothermal Power Plant for Wayang Windu Project, Indonesia. *Proceedings World Geothermal Congress 2000*, Kyushu-Tohoku, Japan, (2000).

Pointon, A. R., T. D., Mills, G. J., Seil, Q., Zhang: Computational Fluid Dynamic Techniques for Validating Geothermal Separator Sizing. *GRC Transactions Vol. 33*: pp. 943 - 948, (2009).

Povarov, O., V., Saakyan, A., Nikolski, V., Luzin, G., Tomarov, M., Saphoznikov: Experience of Creation and Operation of Geothermal Power Plants at Mutnovsky Geothermal Field, Kamchatka, Russia. *International Geothermal Conference, Reykjavic*, (2003).

Povarov, O. A., A.I., Nikolsky: Experience of Creation and Operation of Geothermal Power Plants in Cold Climate Conditions. *Proceedings World Geothermal Congress*, Antalya, Turkey, (2005).

Povarov, O. A. and A. I. Nikolskiy. Modern Russian Geothermal Energy Technologies. *International Geothermal Workshop. Russia*, (2003).

Soeparjadi, R., G. D., Horton, E., Bradley, P. E., Wendt: A Review of the Gunung Salak Geothermal Expansion Project. *Proceedings 20th NZ Geothermal Workshop, New Zealand*, (1998).

Syah, Z., J., Kajo, Z., Antro, M. R.. Raharjo: Project Development of the Wayang Windu Unit 2 Geothermal Power Plant. *Proceedings World Geothermal Congress 2010, Bali, Indonesia*.

Thome, J. R. (2010) *Wolverine Heat Transfer Engineering Data Book III*. (2010).

Thorolfsson, G.: Maintenance History of a Geothermal Plant: Svartsengi Iceland. *Proceedings World Geothermal Congress 2005*, Antalya, Turkey, (2005).

Vargaftic, N. B., B. N.. Volkov, L. D., Voljak: International Tables of the Surface Tension of Water. *J. Phys. Chem. Ref. Data Vol. 12 (No. 3)*: 817 – 820, (1983).

White, B. R.: *The Performance of the Bottom Outlet Cyclone Separators (Wairakei-Type)*. Project Report of Geothermal Institute, University of Auckland, New Zealand. No. 83.27, (1983).